Translational invariance in turbulent cascade models

Martin Greiner,[1] Jens Giesemann,[1,2] and Peter Lipa[3,4]
[1]*Institut für Theoretische Physik, Technische Universität, D-01062 Dresden, Germany*
[2]*Institut für Theoretische Physik, Justus Liebig Universität, D-35392 Gießen, Germany*
[3]*Institut für Hochenergiephysik der Österreichischen Akademie der Wissenschaften, Nikolsdorfergasse 18, A-1050 Vienna, Austria*
[4]*Max-Planck-Institut für Physik komplexer Systeme, D-01187 Dresden, Germany*
(Received 9 May 1997)

Due to the underlying hierarchical structure, spatial correlation functions calculated from multiplicative cascade models are not translationally invariant. A scheme is presented that restores translational invariance by averaging over the experimentally unknown spatial location of cascade realizations with respect to the observation window. The impact of this scheme on multiplier distributions for the energy dissipation field in fully developed turbulence is analyzed; only the experimental multiplier distribution is found to be invariant under a wide range of scales. [S1063-651X(97)14510-X]

PACS number(s): 47.27.−i, 05.40.+j, 02.50.Sk

I. INTRODUCTION

Fully developed turbulence remains a challenging puzzle. To our knowledge no analytic derivation of the intricate fluctuations in the velocity or energy dissipation field has been given from first principles, i.e., the Navier-Stokes equation, although some recent approaches [1] appear to be promising. Astonishingly, many features of experimental observations are also found in simple heuristic models, which thus may be taken as a basis to develop a better phenomenological and mathematical understanding of turbulence. Among these models are, for example, a variety of multiplicative cascade models (or weight-curdling models) [2–5], diffusion models [6,7], the She-Leveque model [8], and approaches based on a Fokker-Planck equation [9].

In this paper we concentrate on multiplicative cascade models [4,5], which successfully capture many statistical features of time series obtained from measurements of the energy dissipation field in fully developed turbulence. In particular, the multifractal analyses, which emphasize the statistics of local singularity strengths, give remarkable good agreement between model predictions and experimental data (see, e.g., [10] and [11] and references therein). Standard multifractal analyses, however, are based on the scaling properties of moments (i.e., integrals over correlation functions) and thus obscure information on the spatial correlations of the energy dissipation field. The latter contain a plethora of additional information and allow us, in principle, to investigate the nature of turbulence on a deeper level.

In two recent papers [12,13] the spatial correlation densities of a general class of multiplicative cascades, including the α model [4] and the p model [5] have been calculated analytically with generating function techniques. Due to the hierarchical organization of the considered cascade models, their spatial correlation functions turn out not to be invariant under spatial translations. This is in clear contrast to experimentally deduced correlation functions that certainly are translationally invariant. This apparent contradiction can be resolved quite easily: for a (one-dimensional) model configuration it is always assumed that the left and right spatial end points of the cascade are known; this means that the ''observation window'' always contains one full cascade, which implies that the observer is able to ''trigger'' a large-eddy structure and record its intrinsic decay. The experimental analysis of recorded time series, which are then interpreted as spatial configurations of the energy dissipation field according to Taylor's frozen hypothesis, does not employ such a trigger. In order to bring model simulations closer to experimental measurement procedures, an averaging over the unknown position of the large scale structures with respect to the observation window needs to be taken into account. Of course, such an averaging scheme destroys the strict self-similarity of the hierarchical cascade models. The question is then, how much? A proper investigation of this point is the subject of this paper.

The organization of the paper is as follows. In Sec. II we briefly review how to calculate spatial correlation functions and their wavelet transforms for multiplicative cascade processes. A simple scheme to restore translational invariance in the correlation functions and in their wavelet transforms is discussed in Sec. III. Basically it uses two independent model configurations of equal lengths, joins them together, and determines the spatial correlations from ''observed'' configurations, which have the same length as each model configuration, but are shifted randomly inside the two adjacent model configurations. We also discuss the case of periodic continuation. In Sec. IV we investigate the impact of this scheme on the so-called multiplier distributions for two specific cascade prescriptions. This is also discussed for a nonhierarchical breakup process and compared to the two previous cases. We summarize the results in Sec. V and give a short outlook.

II. SPATIAL CORRELATIONS IN RANDOM MULTIPLICATIVE PROCESSES

As a prototype for a random multiplicative process the p-model cascade [5] empirically describes the multifractal spectrum of intermittent fluctuations occurring in the energy dissipation of fully developed turbulence. It is described as follows: An energy (dissipation) $E_{00}=1$ distributed uniformly over an interval [0,1] splits into a part $E_{10}=pE_{00}$

contained in the subinterval [0,1/2] and into the remaining part $E_{11}=(1-p)E_{00}$ in [1/2,1]. The random weight p can take the values $(1+\alpha)/2$ or $(1-\alpha)/2$ with equal probability. This is already the splitting prescription for the first step. It is then iterated over all subintervals for the next cascade steps; in each breakup the random number p is tossed independently from all other branchings. After J cascade steps we arrive at 2^J subintervals (bins) of length $1/2^J$ containing the energy densities $\epsilon_{Jk}=E_{Jk}2^J$, where the bins at scale J are indexed by $0\leqslant k<2^J$. After 10–12 cascade steps each p-model configuration shows a striking similarity to the intermittent spatial fluctuations of the energy dissipation measured in fully developed turbulence. A multifractal analysis, which quantifies the singularity strengths of the energy dissipation field, further supports cascade models, as it is in accordance with one-dimensional data [10,11]. However, a closer look at true spatial correlation functions is in demand. If not only the multifractal spectrum, but also the spatial correlation densities of the first few orders (say fourth or fifth order), match the observed data reasonably well, the processes are for all practical purposes indistinguishable.

To determine the spatial correlation densities it is most convenient to use the generating function

$$Z[\lambda]=\left\langle \exp\left(i\sum_{k=0}^{2^J-1}\lambda_k\epsilon_{Jk}\right)\right\rangle, \tag{1}$$

where the bracket $\langle\cdots\rangle$ indicates an averaging over all possible p-model configurations. The correlation densities follow by taking adequate derivatives with respect to the conjugate variables λ_k:

$$\rho_{k_1,\ldots,k_q}=\langle\epsilon_{Jk_1}\cdots\epsilon_{Jk_q}\rangle=\frac{1}{i^q}\frac{\partial^q Z[\lambda]}{\partial\lambda_{k_1}\cdots\partial\lambda_{k_q}}\bigg|_{\lambda=0}, \tag{2}$$

where q represents the order of the correlation function.

The generating function for the p model satisfies a backward evolution equation [12]

$$Z^{(j)}[\lambda^{(j)}]=\int p(q)Z^{(j-1)}[(1+q)\lambda_L^{(j-1)}]\times Z^{(j-1)}[(1-q)\lambda_R^{(j-1)}]\,dq, \tag{3}$$

with the definitions

$$\lambda^{(j)}=(\lambda_0^{(j)},\ldots,\lambda_{2^j-1}^{(j)}),$$
$$\lambda_L^{(j-1)}=(\lambda_0^{(j)},\ldots,\lambda_{2^{j-1}-1}^{(j)}),$$
$$\lambda_R^{(j-1)}=(\lambda_{2^{j-1}}^{(j)},\ldots,\lambda_{2^j-1}^{(j)}), \tag{4}$$

the splitting function

$$p(q)=\frac{1}{2}\delta(q-\alpha)+\frac{1}{2}\delta(q+\alpha), \tag{5}$$

and the initial condition

$$Z^{(0)}[\lambda^{(0)}]=\exp(i\lambda_0^{(0)}). \tag{6}$$

Once this evolution equation is inserted into Eq. (2), recursive relations for the correlation densities $\rho_{k_1,\ldots,k_q}$ can be derived and solved. This has been explicitly demonstrated for the p model in Ref. [12] and extended to a more general class of cascade models with different splitting functions in Ref. [13]. A forward evolution equation allows further generalizations to multiplicative cascades with overlapping branches [14]. Hence, for the p model we merely restate the backward recursion relations for the correlation densities of second order:

$$\rho_{k_1k_2}^{(j)}=\begin{cases}(1+\alpha^2)\rho_{k_1,k_2}^{(j-1)} & \text{for } 0\leqslant k_1,k_2<2^{j-1},\\ (1+\alpha^2)\rho_{k_1-2^{j-1},k_2-2^{j-1}}^{(j-1)} & \text{for } 2^{j-1}\leqslant k_1,k_2<2^j,\\ (1-\alpha^2) & \text{for } 0\leqslant k_1<2^{j-1},\\ & \text{and } 2^{j-1}\leqslant k_2<2^j,\\ & \text{or vice versa.}\end{cases} \tag{7}$$

The construction of $\rho_{k_1k_2}^{(J)}$ by iteration becomes complete by noting that $\rho_{00}^{(0)}=1$.

Figure. 1(a) depicts the two-bin correlation density $\rho_{k_1k_2}$ after six p-model cascade steps for $0\leqslant k_1,k_2<2^6=64$. The power-law rise $(1+\alpha^2)^j$ towards the diagonal is an indication of the self-similarity of the hierarchical p-model cascade: the closer two bins are together, the more they share a common (cascade) history and the stronger they are correlated. For more details consult Ref. [12].

From Fig. 1(a) it is obvious that the second-order correlation density $\rho_{k_1k_2}$ of the p model is not translationally invariant, i.e.,

$$\rho_{k_1k_2}\neq\rho_{k_1+\Delta k,k_2+\Delta k}. \tag{8}$$

We find, for example, that according to Eq. (7) the correlation between two adjacent bins at the lower edge of the interval [0,1], i.e., the bins with labels $k_1=0$ and $k_2=1$, takes the maximal possible value $\rho_{01}^{(J)}=(1+\alpha^2)^{J-1}(1-\alpha^2)$; those two bins share a long cascade history, as they split only in the very last cascade step. On the other hand, the correlation between the two adjacent bins in the very center of [0,1] takes the smallest possible value $\rho_{2^{J-1}-1,2^{J-1}}=(1-\alpha^2)$; these two bins already become independent after the very first cascade step. We emphasize that this strong dependence of the correlation between adjacent bins on their position in the observation interval is not an artifact of the p model, but rather due to the strictly hierarchical organization of cascade processes with nonoverlapping branches in general. In other words, it is the property that larger eddies have of feeding their energy only to offsprings within their boundaries that renders the correlation densities not invariant under translations. This stands in clear contradiction with the experimental results. In the next section we attempt to resolve this puzzle.

So far the representation of the correlation densities is based on a monoscale expansion of the p-model configurations; consult the first row of Fig. 2. The bin correlation densities can be thought of as the correlations between the amplitudes ϵ_{Jk} of this expansion. Clearly, this monoscale

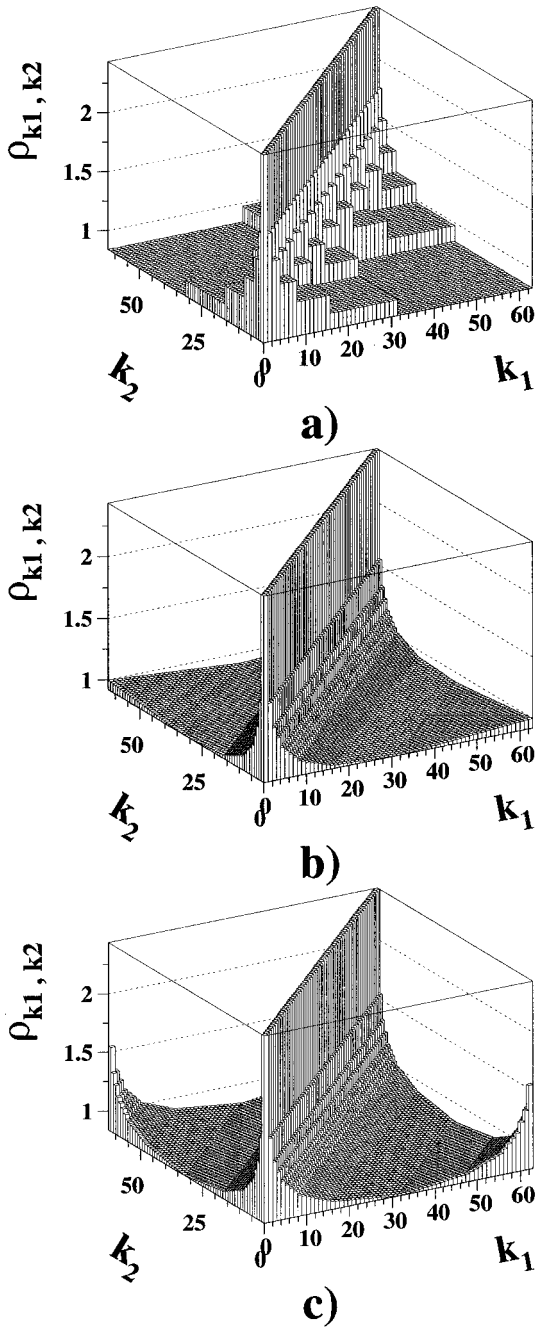

FIG. 1. Two-bin correlation density $\rho_{k_1 k_2}$ for (a) the original p model, (b) the p model made translationally invariant with two independent configurations, and (c) the p model made translationally invariant with two identical configurations. Parameters have been chosen as $J=6$ and $\alpha=0.4$.

representation of the correlation functions is not an optimal choice for a hierarchically organized process like the p-model cascade. A multiscale representation is certainly a better choice. Such a multiresolution expansion can be easily motivated by the successive spatial splittings of the p-model cascade, which become finer in scale as the number of cascade steps increases; it is illustrated in the lower part of Fig. 2. Both the monoscale as well as the multiscale representations each completely characterize a p-model configuration.

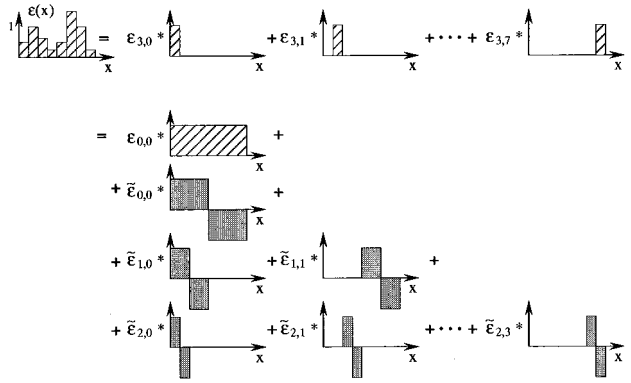

FIG. 2. Monoscale bin representation (first row) and multiscale Haar-wavelet representation (second to fifth rows) of one p-model configuration obtained after $J=3$ cascade steps.

The amplitudes $\tilde{\epsilon}_{jk}$ of the latter are related to the bin amplitudes ϵ_{Jk} of the former by a linear transformation **W**. This transformation is called a Haar-wavelet transformation. We then ask for the correlations

$$\tilde{\rho}_{(j_1 k_1)\ldots(j_q k_q)} = \langle \tilde{\epsilon}_{j_1 k_1} \cdots \tilde{\epsilon}_{j_q k_q} \rangle$$

between the Haar-wavelet amplitudes $\tilde{\epsilon}_{jk}$. These wavelet correlations are determined by employing the wavelet transformation **W** either within the exponent of the generating function (1) or directly to the bin correlation densities (2); for more details see Refs. [12,13].

Figure 3(a) depicts the second-order Haar-wavelet correlations of the p-model cascade. The 2^J wavelet amplitudes have been ordered according to

$$(\epsilon_{00}, \tilde{\epsilon}_{00}, \tilde{\epsilon}_{10}, \tilde{\epsilon}_{11}, \tilde{\epsilon}_{20}, \ldots, \tilde{\epsilon}_{J-1,2^{J-1}-1}).$$

It is diagonal. In other words, the Haar-wavelet transformation completely ''compresses'' the second-order correlation information to the diagonal. Moreover, the diagonal elements $\tilde{\rho}_{(jk)^2} = \alpha^2(1+\alpha^2)^j$ reveal the same power-law scaling as observed in the conventional two-bin correlation density towards the diagonal, and in this way signal the self-similarity of the underlying process.

Thus the representation of the correlation densities is facilitated tremendously once a wavelet transformation is employed: the diagonalization of the covariance matrix shows that the Haar wavelets represent convenient normal coordinates for binary multiplicative cascade models. We note that the higher-order correlation densities are also compressed, and the few nonvanishing contributions provide direct information about hierarchical clustering, i.e., on the correlations of small structures (''eddies'') with their predecessors at larger scales [13,15].

III. RESTORATION OF TRANSLATIONAL INVARIANCE

In the preceding section we stated that the spatial correlation densities of the p model, in particular, and of the binary multiplicative cascade models, in general, are not translational invariant due to their hierarchical spatial organization. This is in clear contradiction to the experimen-

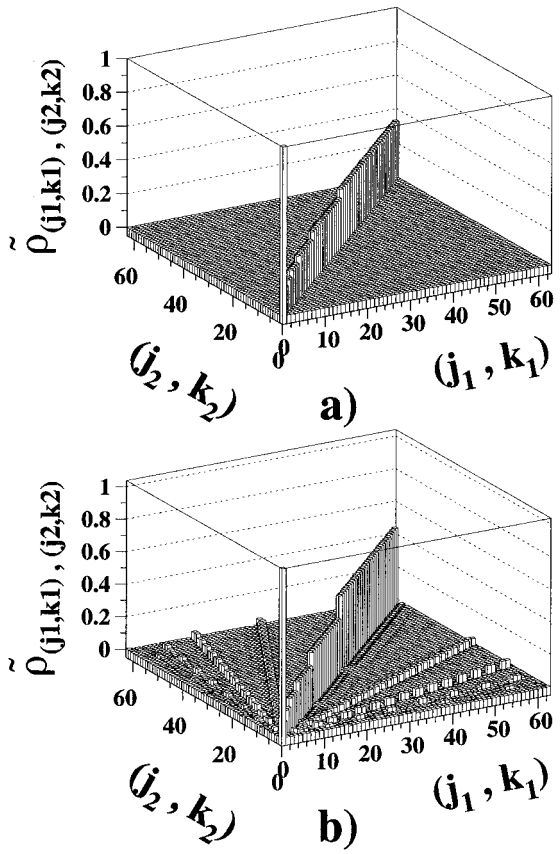

FIG. 3. Haar-wavelet transformed correlation density $\tilde{\rho}_{(j_1k_1),(j_2k_2)}$ of (a) Fig. 1(a) and (b) Fig. 1(b).

tal observations. The reason for this is obvious: in calculating the correlations for the various models we always keep the branching tree at the same position with respect to the observation window; its beginning starts at the left end and stops at the right end of a cascade configuration. However, if we were to measure a time series, which is then identified with a ''spatial configuration'' according to what is known as Taylor's frozen hypothesis, we would not know anything about the spatial location of a ''true'' configuration. This lack of knowledge suggests the introduction of an additional averaging of the spatial correlation densities obtained from hierarchical cascade models over the unknown position of the branching tree with respect to the observation window. In Sec. III A we present a simple averaging scheme to restore translational invariance, based on two independent p-model configurations; in Sec. III B we briefly discuss some modifications of this scheme.

A. Scheme with two independent configurations

We consider one arbitrary configuration μ_1 of the p model obtained after J cascade steps; it has 2^J bins with energy densities $\epsilon_k(\mu_1)$, where $0 \leqslant k < 2^J$. From now on we omit the index J for the energy densities, i.e., $\epsilon_{Jk} \equiv \epsilon_k$. We choose a second, again arbitrary p-model configuration μ_2 of equal length, but which is independent of the former; it goes with energy densities $\epsilon_k(\mu_2)$. Both configurations are joined together and constitute one auxiliary configuration

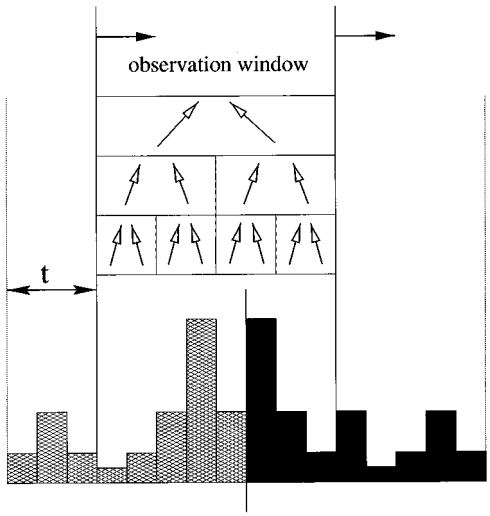

FIG. 4. An observation window is moved bin by bin over two independent p-model configurations ($J=3$, $\alpha=0.4$) and in this manner restores the translational invariance of the spatial correlation densities.

$\mu_1\mu_2$ with 2^{J+1} bins and energy densities $\epsilon_k(\mu_1\mu_2)=\epsilon_k(\mu_1)$ for $0 \leqslant k < 2^J$ and $\epsilon_k(\mu_1\mu_2)=\epsilon_{k-2^J}(\mu_2)$ for $2^J \leqslant k < 2^{J+1}$. Then an observation window of a length corresponding to 2^J bins is moved bin by bin over the auxiliary configuration; see Fig. 4. There are 2^J different positions for the observation window. Each adjustment can be thought of as an ''experimental'' p-model configuration because the beginning (and end) of a ''true'' p-model configuration is not matched, in general; it goes with energy densities $\epsilon_k(t,\mu_1\mu_2)=\epsilon_{k+t}(\mu_1\mu_2)$ with $0 \leqslant k < 2^J$, which of course depend on the position $0 \leqslant t < 2^J$ of the observation window and the two independent p-model configurations $\mu_1\mu_2$. In order to determine the spatial correlation densities we now have to sample over all t and $\mu_1\mu_2$:

$$\langle \rho_{k_1} \rangle_t = \frac{1}{2^J} \sum_{t=0}^{2^J-1} \sum_{\mu_1\mu_2} p_{\mu_1\mu_2} \epsilon_{k_1+t}(\mu_1\mu_2) = \langle \langle \epsilon_{k_1} \rangle_{\mu_1\mu_2} \rangle_t ,$$

$$\langle \rho_{k_1k_2} \rangle_t = \frac{1}{2^J} \sum_{t=0}^{2^J-1} \sum_{\mu_1\mu_2} p_{\mu_1\mu_2} \epsilon_{k_1+t}(\mu_1\mu_2) \epsilon_{k_2+t}(\mu_1\mu_2) = \langle \langle \epsilon_{k_1} \epsilon_{k_2} \rangle_{\mu_1\mu_2} \rangle_t \ , \ldots . \quad (9)$$

The inner bracket $\langle\ \rangle_{\mu_1\mu_2}$ indexed with $\mu_1\mu_2$ is a shorthand notation for the averaging over all independent p-model configurations μ_1 and μ_2, which occur with the probability $p_{\mu_1\mu_2}=p_{\mu_1}p_{\mu_2}$. The outer bracket $\langle\ \rangle_t$ indexed with the position label t indicates an averaging over all possible positions of the observation window. By construction, the spatial correlation densities $\langle \rho_{k_1,\ldots,k_q} \rangle_t$ are translationally invariant.

The first-order correlation density $\langle \rho_{k_1} \rangle_t$ is easy to calculate, because $\epsilon_{k_1+t}(\mu_1\mu_2)$ depends on only one of the two configurations $\mu=\mu_1$ or $\mu=\mu_2$:

$$\langle \rho_{k_1} \rangle_t = \frac{1}{2^J} \sum_{t=0}^{2^J-1} \sum_{\mu} p_\mu \epsilon_{k_1+t}(\mu) = \frac{1}{2^J} \sum_{t=0}^{2^J-1} \rho_{k_1+t} = \rho_{k_1} = 1, \tag{10}$$

because the one-bin correlation density $\rho_{k_1+t}=\rho_{k_1}$ does not depend on the position parameter, and for the energy-conserving p model we have $\rho_{k_1}=1$ for all $0 \leqslant k_1 < 2^J$.

For the second-order correlation density $\langle \rho_{k_1 k_2} \rangle_t$ we have to be more careful:

$$\begin{aligned} \langle \rho_{k_1 k_2} \rangle_t &= \frac{1}{2^J} \sum_{t=0}^{2^J-1} \sum_{\mu_1 \mu_2} p_{\mu_1 \mu_2} \epsilon_{k_1+t}(\mu_1 \mu_2) \epsilon_{k_2+t}(\mu_1 \mu_2) \\ &\equiv \frac{1}{2^J} \sum_{t=0}^{2^J-1} \rho_{k_1+t,k_2+t}. \end{aligned} \tag{11}$$

Two major cases have to be distinguished: for $0 \leqslant k_1, k_2 < 2^J - t$ (or $2^J - t \leqslant k_1, k_2 < 2^J$) the two energy densities ϵ_{k_1} and ϵ_{k_2} belong to the same ''true'' p-model configuration $\mu=\mu_1$ (or $\mu=\mu_2$) and we have

$$\begin{aligned} \rho_{k_1+t,k_2+t} &= \sum_{\mu} p_\mu \epsilon_{k_1+t}(\mu) \epsilon_{k_2+t}(\mu) \\ &= \begin{cases} \rho_{k_1+t,k_2+t} & \text{for } \mu=\mu_1 \\ \rho_{k_1+t-2^J,k_2+t-2^J} & \text{for } \mu=\mu_2 \end{cases}. \end{aligned} \tag{12}$$

For these two cases the translated correlation density ρ_{k_1+t,k_2+t} is directly expressible in terms of the true p-model correlation densities $\rho_{k_1' k_2'}$. Still, we have to consider the case $0 \leqslant k_1 < 2^J - t$ and $2^J - t \leqslant k_2 < 2^J$ (or vice versa). Then ϵ_{k_1} and ϵ_{k_2} belong to two different ''true'' p-model configurations, which are independent of each other; hence, we deduce

$$\begin{aligned} \rho_{k_1+t,k_2+t} &= \left(\sum_{\mu_1} p_{\mu_1} \epsilon_{k_1+t}(\mu_1) \right) \left(\sum_{\mu_2} p_{\mu_2} \epsilon_{k_2+t}(\mu_2) \right) \\ &= \rho_{k_1+t} \cdot \rho_{k_2+t-2^J} = 1. \end{aligned} \tag{13}$$

Equations (11)–(13) are illustrated in Fig. 5 and represent our recipe to determine translational invariant correlation densities (of second order). In Sec. III B we will also discuss some variations of this approach.

Following Eqs. (11)–(13), the second-order spatial correlation density $\langle \rho_{k_1 k_2} \rangle_t$ for the p model is shown in Fig. 1(b). By construction it is translational invariant, i.e., $\langle \rho_{k_1 k_2} \rangle_t = \langle \rho_{k_1+\Delta k, k_2+\Delta k} \rangle_t$. It reveals a minimum of $\langle \rho^{(J)}_{0+\Delta k, 2^{J-1}+\Delta k} \rangle_t = \frac{1}{2}[1+(1-\alpha^2)]$ at a line parallel to the diagonal with a (bin) distance of 2^{J-1}; it occurs due to the energy-conserving anticorrelation $\rho_{k_1, k_2+2^{J-1}} = 1-\alpha^2$ with $0 \leqslant k_1, k_2 < 2^{J-1}$ of the original p model and due to the independence of the two true p-model configurations employed for the scheme to restore translational invariance. The scaling behavior of $\langle \rho_{k_1 k_2} \rangle_t$ perpendicular to the diagonal is not dramatically altered.

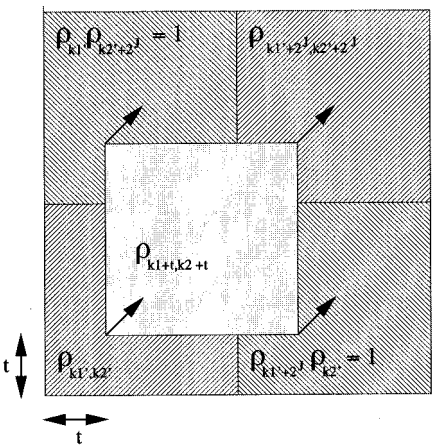

FIG. 5. The auxiliary second-order correlation density matrix is based on two independent p-model correlations. The diagonal blocks $\rho_{k_1' k_2'}$ and $\rho_{k_1'+2^J, k_2'+2^J}$ are identical to the second-order correlation density of the p model; see Fig. 1(a). The two off-diagonal blocks are decorrelated, so that each element is equal to 1. ρ_{k_1+t,k_2+t} represents the translated correlation density based on measurements in the observation window of Fig. 4. The translationally invariant correlation density $\langle \rho_{k_1 k_2} \rangle_t$ is obtained by averaging over shifts along the diagonal from the lower left corner of the auxiliary matrix to the upper right corner.

This also becomes clear once we investigate the box moments

$$M_q(j) = \frac{1}{2^j} \sum_{k=0}^{2^j-1} \frac{1}{2^{q(J-j)}} \sum_{k 2^{J-j} \leqslant k_1, \ldots, k_q < (k+1) 2^{J-j}} \rho^{(J)}_{k_1, \ldots, k_q}, \tag{14}$$

which represents averages of the correlation density $\rho^{(J)}_{k_1, \ldots, k_q} = \rho_{k_1, \ldots, k_q}$ of order q over boxes with a scale-dependent bin size of 2^{J-j}. For $q=2$ they are depicted in Fig. 6; it only deviates to some minor extent from the perfect p-model scaling $(1+\alpha^2)^j$.

For the original p model the Haar wavelets represent the perfect building blocks (normal coordinates); the Haar-wavelet transformation leads to a perfect diagonalization of the spatial correlation density of second order [see Fig. 3(a)]. This is not the case for the translationally invariant correlation density $\langle \rho_{k_1 k_2} \rangle_t$; its Haar-wavelet transform is shown in Fig. 3(b). Although it is not diagonal anymore, it is still quasidiagonal in a very pronounced way: diagonal elements of $\langle \tilde{\rho}_{k_1 k_2} \rangle_t = \Sigma_{k_3, k_4} \mathbf{W}_{k_1 k_3} \mathbf{W}_{k_2 k_4} \langle \rho_{k_3 k_4} \rangle_t$ dominate the off-diagonal elements, which mainly occur in interscale bands. Hence, we conclude that as ''quasi'' building blocks of the translationally invariant p model the Haar wavelets still appear to be fairly good approximations to the ''true'' normal coordinates.

The scale dependence of the diagonal elements, i.e.,

$$W_q(j) = \frac{1}{2^j} \sum_{k=0}^{2^j-1} \tilde{\rho}_{(jk)^q}, \tag{15}$$

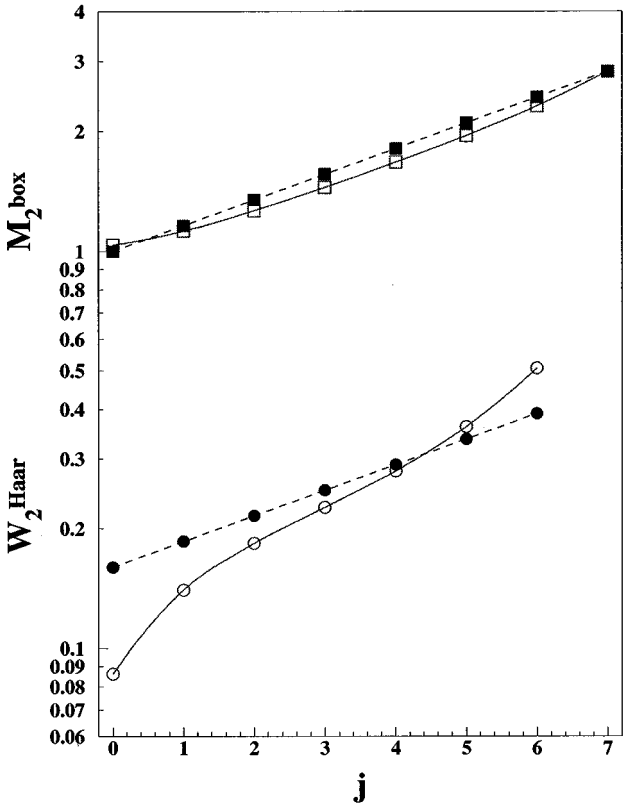

FIG. 6. Dependence of the box moments (squares) and Haar-wavelet moments (circles) of order $q=2$ on the resolution scale j for the original p model (dashed lines) and the p model with restoration of translational invariance using two independent configurations (solid lines). Parameters are $J=7$ and $\alpha=0.4$.

is depicted in the lower part of Fig. 6. Here, even for $q=2$ the scheme to restore translational invariance leads to sizable deviations from the p model's perfect scaling $\tilde{\rho}_{(jk)^q}=\alpha^2(1+\alpha^2)^j$, in particular at the roughest (small j) and finest (large j) scales. The reason for this is, once again, that the wavelet amplitudes $\tilde{\epsilon}_{jk}$ represent local differences instead of local averages; hence they are much more sensitive to the nature of the fluctuations occurring in the ''experimental'' p-model configurations.

B. Modified schemes

In the preceding section we have used two independent p-model configurations to restore the translational invariance of the covariance matrix $\rho_{k_1k_2}$. Mathematically it is also interesting to study the case of periodic p-model configurations; here we could think of a one-dimensional p model as represented on a ring, where the beginning and the end of a configuration are connected. This scenario occurs, for example, in high energy physics when two-dimensional particle density fields are studied in the coordinates (η,Φ), where η is the particle's (pseudo)rapidity and Φ its azimuthal angle with respect to the collision axis. The overall procedure with periodic configurations is the same as with two independent ones presented in Sec. III A. Only some minor technicalities have to be changed. First, of course, the second p-model configuration shown in Fig. 4 has to be identical to the first one. The general relations (9) still hold with $\mu_1=\mu_2$ and $p_{\mu_1\mu_2}=p_{\mu_1}$, as does Eq. (10) for the first-order correlation density; i.e., again $\langle\rho_{k_1}\rangle_t=1$ for all k_1. Figure 5 has to be modified: the two off-diagonal blocks become identical to the diagonal blocks, so that now each of the four submatrices corresponds to one ''true'' p-model correlation density $\rho_{k_1k_2}$ of second order. As a consequence, Eq. (12) remains unaltered, whereas Eq. (13) changes into

$$\rho_{k_1+t,k_2+t}=\rho_{k_1+t,k_2+t-2^J} \tag{16}$$

for $0\leqslant k_1<2^J-t$, $2^J-t\leqslant k_2<2^J$ and

$$\rho_{k_1+t,\,k_2+t}=\rho_{k_1+t-2^J,k_2+t} \tag{17}$$

for $2^J-t\leqslant k_1<2^J$, $0\leqslant k_2<2^J-t$. Insertion of Eqs. (12), (16), and (17) into Eq. (11) yields the translational invariant second-order correlation density $\langle\rho_{k_1k_2}\rangle_t$ obtained with two identical p-model configurations; it is depicted in Fig. 1(c). It shows an approximate power-law decrease perpendicular to the diagonal until the minimum at $\langle\rho_{\Delta k,2^{J-1}+\Delta k}\rangle_t=1-\alpha^2$ with $0\leqslant\Delta k<2^J$ is reached at a bin distance of 2^{J-1} from the diagonal. For larger bin distances the second-order correlation density increases again; it is reflection symmetric around its minimum line due to the periodic continuation of one p-model configuration (equal to two identical configurations).

Many other schemes to restore translational invariance of spatial correlation densities can be constructed. For example, we could return to the scheme with two (or more) independent p-model configurations of equal length and change the size of the observation window (''experimental'' configuration) to be smaller or larger than one p-model configuration. In the first case we would arrive at a submatrix of $\langle\rho_{k_1k_2}\rangle_t$; also, in the second case $\langle\rho_{k_1k_2}\rangle_t$ is identical to the result depicted in Fig. 1(b), except for the long range bin correlations with $|k_1-k_2|\geqslant 2^J$, where $\langle\rho_{k_1k_2}\rangle_t=1$ due to the assumed independence of the multiple p-model configurations of bin length 2^J each. From an ''experimental'' point of view, this onset of decorrelation in the spatial correlation functions for large bin distances is a tool for determining the relevant length scales of the cascade regime.

IV. MULTIPLIER DISTRIBUTIONS

We now investigate the influence of our scheme to restore translational invariance in the spatial correlation densities on the so-called multiplier distributions. The latter represent a much better opportunity to compare theoretical models with experimental results than a scaling analysis, as they are more directly related to the splitting function of the (assumed) underlying cascade process [see Eqs. (3) and (5)]. In Sec. IV A we work again with the p-model splitting function, whereas in Sec. IV B we concentrate on a splitting function obtained empirically by Sreenivasan and Stolovitzky [11]. For further support of the conclusions to be drawn we also investigate a nonhierarchical breakup process in Sec. IV C.

A. *p*-model multiplier distributions

We have another close look at the evolution of one p-model configuration; consult again the beginning of Sec. II. For an arbitrary cascade step $j \to j+1$ the energies evolve as

$$E_{2k}^{(j+1)} = W_{\pm}^{(j)} E_k^{(j)},$$

$$E_{2k+1}^{(j+1)} = W_{\mp}^{(j)} E_k^{(j)}, \tag{18}$$

with $0 \leqslant k < 2^j$, where $W_{\pm}^{(j)}$ are called multipliers and take on two values, i.e., $W_{\pm}^{(j)} = (1 \pm \alpha)/2$. In terms of energy densities, Eq. (18) translates into

$$\epsilon_{2k}^{(j+1)} = 2 W_{\pm}^{(j)} \epsilon_k^{(j)},$$

$$\epsilon_{2k+1}^{(j+1)} = 2 W_{\mp}^{(j)} \epsilon_k^{(j)}. \tag{19}$$

Given now one p-model configuration, we can identify the ''splitting weight'' α entering the multiplier according to

$$\frac{\epsilon_{2k}^{(j+1)} - \epsilon_{2k+1}^{(j+1)}}{\epsilon_{2k}^{(j+1)} + \epsilon_{2k+1}^{(j+1)}} = \frac{W_{\pm}^{(j)} - W_{\mp}^{(j)}}{W_{\pm}^{(j)} + W_{\mp}^{(j)}} = \pm \alpha. \tag{20}$$

Consequently, we arrive at the ''experimental'' probability density of the splitting parameter q,

$$p(q) = \frac{1}{2}\delta(q-\alpha) + \frac{1}{2}\delta(q+\alpha), \tag{21}$$

which is exactly equal to the splitting function (5) of the energy-conserving p model. Again, for the original p model the latter depends neither on scale j nor on localization k.

This is going to change once we consider the scheme (with two independent p-model configurations) depicted in Fig. 4 to restore translational invariance in the spatial correlation densities. The probability density for the splitting parameter is determined in the following way: we select two arbitrary and independent p-model configurations μ_1 and μ_2, each obtained after J cascade steps, join them together, and choose an observation window of bin length 2^J at position t; consult Fig. 4. We then have one ''experimental'' p-model configuration with energy densities $\epsilon_{k+t}(\mu_1\mu_2) \equiv \epsilon_{k+t}^{(J)}(\mu_1\mu_2) \equiv \epsilon_k^{(J)}(t,\mu_1\mu_2)$, where $0 \leqslant k < 2^J$. We think of this configuration as a p-model-like configuration as we force it into a spatially dyadic scheme, where we operate with the (backward) energy-conserving smoothings

$$\epsilon_k^{(j)}(t,\mu_1\mu_2) = \frac{1}{2}[\epsilon_{2k}^{(j+1)}(t,\mu_1\mu_2) + \epsilon_{2k+1}^{(j+1)}(t,\mu_1\mu_2)] \tag{22}$$

with $0 \leqslant j < J$. Then, analogously to Eq. (20), we determine the splitting parameters $\alpha_k^{(j)}(t,\mu_1\mu_2)$ by

$$\alpha_k^{(j)}(t,\mu_1\mu_2) = \frac{\epsilon_{2k}^{(j+1)}(t,\mu_1\mu_2) - \epsilon_{2k+1}^{(j+1)}(t,\mu_1\mu_2)}{\epsilon_{2k}^{(j+1)}(t,\mu_1\mu_2) + \epsilon_{2k+1}^{(j+1)}(t,\mu_1\mu_2)}. \tag{23}$$

This holds for one t and one choice $\mu_1\mu_2$; we then have to average over all positions $0 \leqslant t < 2^J$ of the observation window and over all double p-model configurations $\mu_1\mu_2$. This is continued recursively in the ''backward'' direction for all scales $J > j \geqslant 0$, starting from scale $j = J-1$ up to the coarsest scale $j = 0$. In this way we obtain for each scale a ''backward'' or ''experimental'' splitting function

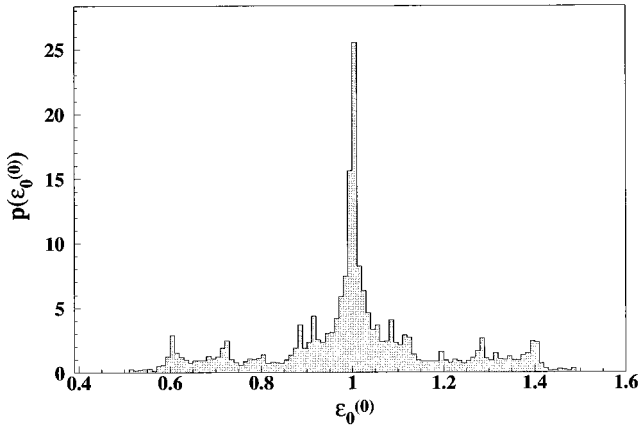

FIG. 7. Probability density $p(\epsilon_0^{(0)})$ of the global energy density $\epsilon_0^{(0)} \equiv \epsilon_0^{(0)}(t,\mu_1\mu_2)$ in the observation window; the latter depends on the translation index t of the observation window and the two independent p-model configurations $\mu = \mu_1\mu_2$. Parameter values are $J=9$ and $\alpha = 0.4$.

$$p^{(j)}(q) = \sum_{\mu_1\mu_2} p_{\mu_1\mu_2} \frac{1}{2^J} \sum_{t=0}^{2^J-1} \frac{1}{2^j} \sum_{k=0}^{2^j-1} \delta(q - \alpha_k^{(j)}(t,\mu_1\mu_2)). \tag{24}$$

This construction is difficult to perform analytically; therefore we sample over N double p-model configurations $\mu_1\mu_2$ and replace $\Sigma_{\mu_1\mu_2} p_{\mu_1\mu_2} \to 1/N \Sigma_{i=1}^{N}$ with $\mu_1\mu_2 = \mu_1(i)\mu_2(i)$. Furthermore, due to the many δ functions appearing in Eq. (24), we divide the interval $-1 \leqslant q \leqslant 1$ into $2M$ cells of length $\Delta q = 1/M$, integrate $p^{(j)}(q)$ over each such cell, and arrive at the discretized probability density function,

$$p^{(j)}(q_m) = \frac{1}{\Delta q} \int_{q_m}^{q_m + \Delta q} \frac{1}{N} \sum_{i=1}^{N} \frac{1}{2^J} \times \sum_{t=0}^{2^J-1} \frac{1}{2^j} \sum_{k=0}^{2^j-1} \delta[q - \alpha_k^{(j)}(t,\mu_1(i)\mu_2(i))] dq, \tag{25}$$

with $q_m = m\Delta q$ and $-M \leqslant m < M$.

Before we present the result for the discretized probability density function we point out one more detail: since the observation window reaches over two independent ''true'' p-model configurations, the total energy accumulated in the observation window will generally not be equal to the initial energy E_{00} of the p model; in other words, $\epsilon_0^{(0)}(t,\mu_1\mu_2) \neq 1$. However, we expect the distribution $p(\epsilon_0^{(0)})$ [where we set $\epsilon_0^{(0)} \equiv \epsilon_0^{(0)}(t,\mu_1\mu_2)$ for brevity] to be narrowly peaked around 1; this behavior is confirmed numerically in Fig. 7. Observe that the prescription (23) for determining the ''ex-

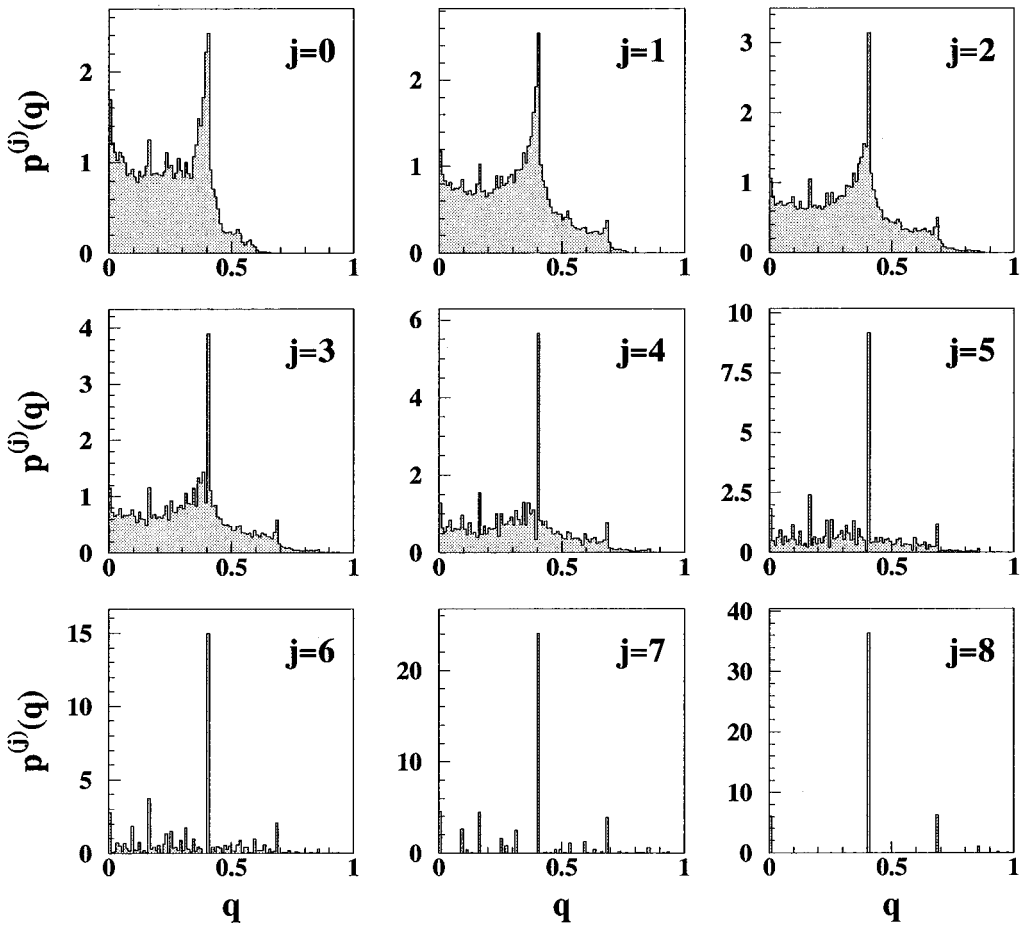

FIG. 8. Scale-dependent probability densities $p^{(j)}(q)$ of the ''experimental'' splitting parameters of the translation invariant p model obtained by averaging over shifts of the observation window over two independent p-model configurations. Parameters have been set to $J=9$ and $\alpha=0.4$.

perimental'' splitting parameters $\alpha_k^{(j)}(t,\mu_1\mu_2)$ is independent of the variability of $\epsilon_0^{(0)}(t,\mu_1\mu_2)$ and, thus, no renormalization is necessary.

Figure 8 illustrates the scale-dependent discretized probability density $p^{(j)}(q)$ of Eq. (25), where the scheme with two independent p-model configurations to restore translational invariance has been employed. We used $J=9$ cascade steps and $\alpha=0.4$, corresponding to $p=(1+\alpha)/2=0.7$ of Ref. [5]. The splitting parameter $-1\leqslant q\leqslant 1$ is related to the multiplier $0\leqslant W\leqslant 1$ by $W=(1+q)/2$; thus, the splitting functions $p^{(j)}(q)$ can also be thought of as ''experimental'' multiplier distributions. They are, by construction, symmetric around $q=0$ (or $W=1/2$, respectively); hence, we only show the part for $q\geqslant 0$. Contrary to the ''true'' p model (without restoration of translational invariance), where $p^{(j)}(q)$ has only two δ-function-like contributions at $q=\pm\alpha$ and is independent of the scale j [see Eq. (5)], the splitting function now shows scale dependence. For large j values only a few pronounced peaks occur in $p^{(j)}(q)$, the dominating ones keeping a slowly decaying memory of the original δ functions at $q=\pm\alpha$; this is easily understood: the energy densities $\epsilon_k^{(j)}(t,\mu_1\mu_2)$ of an ''experimental'' p-model configuration, which consists of two independent realizations of true p-model configurations obtained after J cascade steps, can only take $J+1$ different values at most, namely $(1+\alpha)^J$, $(1+\alpha)^{J-1}(1-\alpha),\ldots,(1+\alpha)(1-\alpha)^{J-1}$, and $(1-\alpha)^J$. Out of these, only a few different ratios of the form (23) can be formed, some of them occurring quite rarely. For the next rougher scales $j<J$, the $\epsilon_k^{(j)}(t,\mu_1\mu_2)$ can take on more than $J+1$ values; see Eq. (22). Hence, for decreasing j more and more possible values of ratios (23) arise, which explains that the probability density $p^{(j)}(q)$ becomes smoother as $j\to 0$. For small j the $p^{(j)}(q)$ even seem to converge and become approximately scale independent.

In view of this result one question naturally arises: how relevant is the p-model splitting function (5) in describing the energy dissipation process in fully developed turbulence? With our scheme to restore translational invariance in the spatial correlation densities we have designed a ''gedanken'' experiment on how an experimentalist would deduce the probability density functions for the splitting weights q, which is trivially related to the multiplier distributions and, with the presumption of energy conservation, to the splitting function. Apparently, these experimental p-model splitting functions are quite different from the original one (5). A dominant peak at $q=\pm\alpha$ is still found on all scales, but also other q values contribute to a large extent; moreover, the experimental p-model splitting function becomes scale-

dependent, in contrast to the original one. In other words, we start with a self-similar cascade model with no translational invariance, then restore translational invariance, but lose self-similarity. Hence, we should pose the above question in another way: can we find a splitting function which stays more or less the same (is stable) as the scheme to restore translation invariance is applied, and how relevant is it in describing real data in fully developed turbulence? In this context it is most natural to look on the experimentally deduced multiplier distributions obtained from real data.

B. Experimental multiplier distributions

Out of one-dimensional time series from fully developed turbulence, Sreenivasan and Stolovitzky (SRST) deduced empirically a largely scale-independent multiplier distribution [11]. A suitable parametrization is given by the β distribution,

$$p_{\mathrm{SRST}}(q)=\frac{1}{2}\frac{\Gamma(2\beta)}{\Gamma(\beta)^2}\left(\frac{1+q}{2}\right)^{\beta-1}\left(\frac{1-q}{2}\right)^{\beta-1}$$

$$=\frac{1}{2^{2\beta-1}}\frac{\Gamma(2\beta)}{\Gamma(\beta)^2}(1-q^2)^{\beta-1}, \qquad (26)$$

where the single parameter $\beta=3.2$ is chosen. This represents a good fit to the empirical multiplier distributions, which are observed to be scale-independent over a wide range of scales [11]; only for the very fine scales (large j) do they deviate and become wider, whereas for the very rough scales (small j) they narrow more towards a δ function at $q=0$.

With a new splitting function like Eq. (26) it is straightforward to calculate the spatial correlation densities. The spatial dyadic structure of the cascade model with the empirically deduced splitting function (26), which we henceforth refer to as a SRST cascade, is identical to the p-model process. Hence, Eqs. (2)–(4), (6), and (26) can be employed. For the construction of the second-order correlation densities we can use the recursion relations (7) with the substitutions $(1+\alpha^2)\rightarrow\int_{-1}^{1}(1+q)^2 p_{\mathrm{SRST}}(q)dq$ and $(1-\alpha^2)\rightarrow\int_{-1}^{1}(1+q)(1-q)p_{\mathrm{SRST}}(q)dq$; for more technical details consult [13]. The two-bin correlation density $\rho_{k_1k_2}$ of the SRST cascade looks the same as for the p-model case depicted in Fig. 1(a); this also holds for the Haar-wavelet transformed correlation densities and the various moments.

The scheme presented in Sec. III A to restore translational invariance with two independent cascade configurations now needs to be modified for one tiny detail: instead of two independent p-model configurations we now choose two inde-

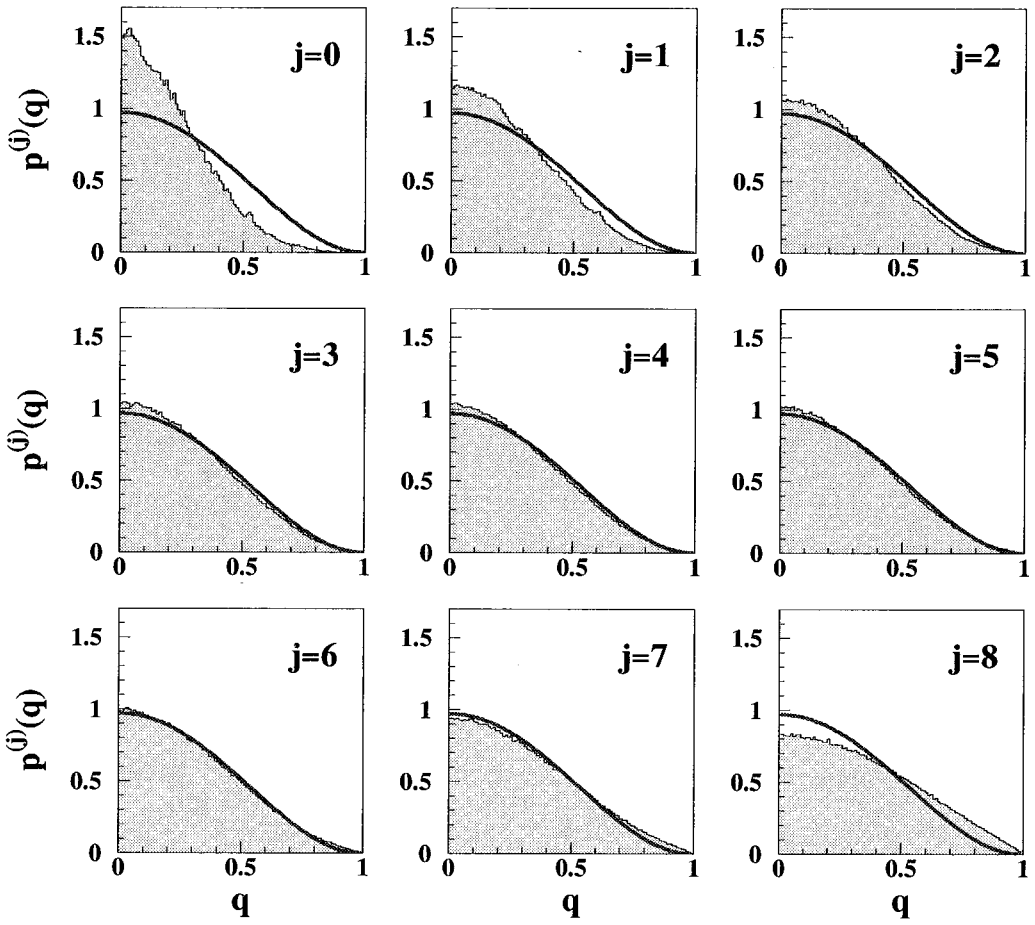

FIG. 9. Scale-dependent probability densities $p^{(j)}_{\mathrm{SRST}}(q)$ of the ''experimental'' splitting parameters of the translation invariant SRST-cascade model obtained by averaging over shifts of the observation window over two independent SRST-cascade configurations. Parameters have been set to $J=9$ and $\beta=3.2$. For comparison, the empirical splitting function $p_{\mathrm{SRST}}(q)$ of Eq. (26) with $\beta=3.2$ is shown as a solid curve.

pendent SRST-cascade configurations; the rest stays the same. Again, the translationally invariant correlation density $\langle \rho_{k_1 k_2} \rangle_t$ for the SRST cascade has the same appearance as the one shown in Fig. 1(b), which has been obtained from the p model; this also holds for the moments and wavelet transformed correlation densities considered [see Figs. 3(b) and 6].

Having in mind the question posed at the end of Sec. IV A, we now focus on the impact of the scheme to restore translational invariance on the ''true'' probability density function $p_{\mathrm{SRST}}(q)$, which can be interpreted either as a multiplier distribution or as a splitting function. We proceed again according to Eq. (25). The results are depicted in Fig. 9. For a large regime of scales (roughly $2 \leqslant j \leqslant 7$) the ''experimental'' $p^{(j)}_{\mathrm{SRST}}(q)$ more or less collapse with the original $p_{\mathrm{SRST}}(q)$ (solid curve). For the very rough scales $j=0,1$ the distributions become narrower around $q=0$, which is also in accordance with the real experimental observations [11]. For the finest scale shown, i.e., $j=8$, the distribution is more flat; this trend also agrees with the real experimental observations [11]. It seems that we have already found what we were looking for: in our simple scheme to restore translational invariance in the turbulent cascade models, the experimentally deduced scale-independent multiplier distribution (26) reproduces itself over many scales. Two conclusions can be drawn: first of all, the simple restoration scheme with two independent cascade configurations appears to be confirmed or at least mimics some relevant truth; second and maybe more far-reaching, the simple cascade models, used hitherto as toy models to describe fluctuations in the energy dissipation process in fully developed turbulence, have obtained a deeper foundation from a phenomenological point of view. We start with a hierarchical, self-similar cascade model with the scale-independent splitting function $p_{\mathrm{SRST}}(q)$, restore the missing translational invariance, and arrive at effective splitting functions $p^{(j)}_{\mathrm{SRST}}(q) \approx p_{\mathrm{SRST}}(q)$, which are quite scale-independent and almost identical to the original one. This finding confirms and extends the main conclusions of Ref. [11] in that the empirically deduced β function has the peculiar property of being stable with respect to our scheme to restore translation invariance.

Before we take this statement to the books we should also check counterexamples. Hence, in Sec. IV C we investigate the multiplier distribution obtained from a nonhierarchical random process.

C. Multiplier distribution of a one-step breakup process

Like the p model the original SRST-cascade model (without restoration of translation invariance) is based on a hierarchical (dyadic) ordering of the energy densities $\epsilon^{(J)}_k(\mu) = \epsilon_{Jk}(\mu)$. The energy densities $\epsilon^{(J)}_{2k}(\mu)$ and $\epsilon^{(J)}_{2k+1}(\mu)$ of two neighboring bins both evolve from the same ''parent'' energy density $\epsilon^{(J-1)}_k$. We now introduce a random process, which produces configurations with the same $\epsilon^{(J)}_k(\mu)$ values, but with a completely random spatial ordering. In practice this means: we take one arbitrary SRST-cascade configuration μ with energy densities $\epsilon^{(J)}_k(\mu)$ assigned to bins $0 \leqslant k < 2^J$; then we randomly permute the k values to obtain a modified configuration that still has

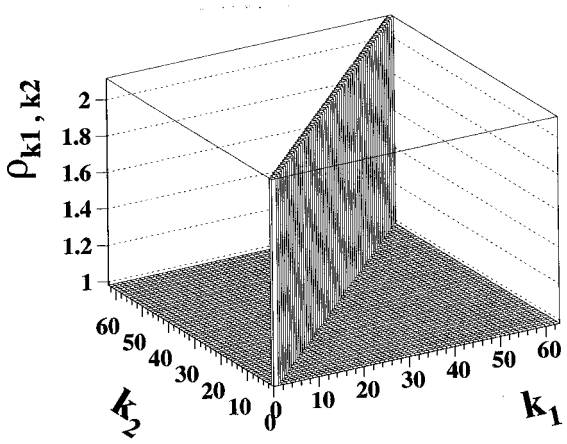

FIG. 10. Two-bin correlation density $\rho_{k_1 k_2}(\mathrm{BP})$ for the spatially randomized SRST-cascade process with $J=6$ and the SRST-splitting function (26) with $\beta = 3.2$.

the same number of spikes and holes but no longer reflects the hierarchical ordering of the cascade process.

After the random permutation of the bin ordering, two neighboring bins with labels $2k$ and $2k+1$ do not share a common history anymore; hence, they become decorrelated. Except for first order, the spatial correlation densities of this random process, which can be viewed as a one-step breakup process (BP), differ drastically from those of the SRST cascade. Again we pick the second order for an illustration. The diagonal elements $\rho^{(J)}_{k_1 k_1}(\mathrm{BP})$ remain the same as for the SRST cascade:

$$\rho^{(J)}_{k_1 = k_2}(\mathrm{BP}) = \left(\int_{-1}^{1} (1+q)^2 p_{\mathrm{SRST}}(q)\, dq \right)^J . \tag{27}$$

The off-diagonal elements are all equal and easy to calculate once we make use of energy conservation:

$$\begin{aligned} 1 &= \langle E^2 \rangle \\ &= \left\langle \left(\frac{1}{2^J} \sum_{k_1=0}^{2^J-1} \epsilon^{(J)}_{k_1} \right) \left(\frac{1}{2^J} \sum_{k_2=0}^{2^J-1} \epsilon^{(J)}_{k_2} \right) \right\rangle \\ &= \frac{1}{2^{2J}} \sum_{k_1, k_2 = 0}^{2^J-1} \rho^{(J)}_{k_1 k_2}(\mathrm{BP}) \\ &= \frac{1}{2^{2J}} [2^J \rho^{(J)}_{k_1 = k_2}(\mathrm{BP}) + 2^J (2^J - 1) \rho^{(J)}_{k_1 \neq k_2}(\mathrm{BP})]; \end{aligned}$$

from here it follows that

$$\rho^{(J)}_{k_1 \neq k_2}(\mathrm{BP}) = \frac{1}{2^J - 1} [2^J - \rho^{(J)}_{k_1 = k_2}(\mathrm{BP})]. \tag{28}$$

The two-bin correlation density $\rho^{(J)}_{k_1 k_2}(\mathrm{BP})$ is shown in Fig. 10. As expected it is completely different from Fig. 1(a), where $\rho_{k_1 k_2}$ of the p model has been depicted, the latter being the same as for the SRST cascade. This obvious dif-

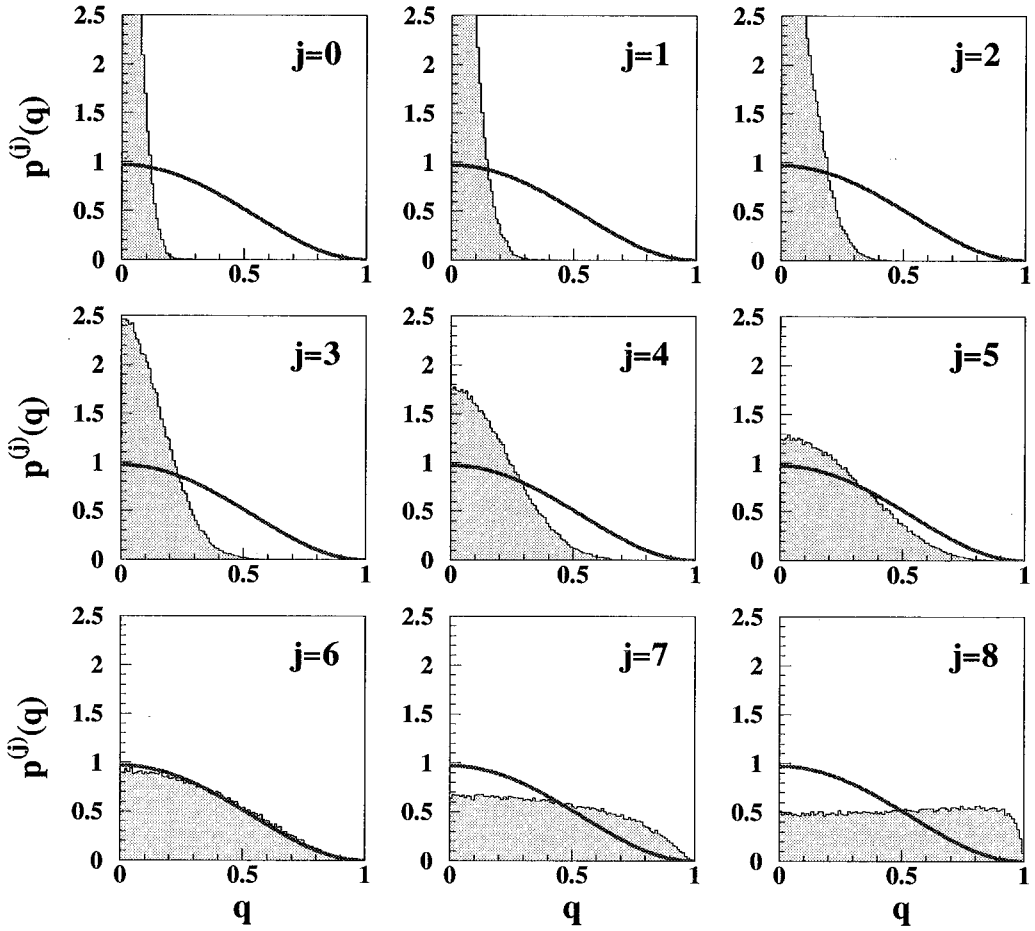

FIG. 11. Scale-dependent multiplier distribution $p_{\mathrm{BP}}^{(j)}(q)$ out of the restoration scheme for translational invariance with two independent, spatially randomized SRST-cascade configurations. Parameters have been set to $J=9$ and $\beta=3.2$. For comparison, the empirical splitting function $p_{\mathrm{SRST}}(q)$ of Eq. (26) with $\beta=3.2$ is shown as a solid curve.

ference still holds once we use our scheme with two independent random configurations to restore translational invariance.

In terms of spatial correlation densities the SRST cascade can be clearly distinguished from the corresponding randomized process. The same is also true for the multiplier distributions $p_{\mathrm{BP}}^{(j)}(q)$ of Eq. (25) once we apply the scheme to restore translational invariance with two independent, now spatially randomized SRST-cascade configurations. The result is illustrated in Fig. 11. No approximate scale invariance and no convergence to the multiplier distribution $p_{\mathrm{SRST}}(q)$ of Eq. (26) (solid line) can be claimed. This outcome further underlines the statements given at the end of Sec. IV B.

V. CONCLUSIONS

We have presented a simple scheme to restore translational invariance in hierarchical multiplicative cascade models: an ''experimental'' configuration is constructed from two independent cascade configurations of equal length, the latter being attached to the former. By randomly shifting the observation window around, the knowledge about the spatial position of individual cascade configurations is lost and, consequently, the spatial correlation functions become invariant under translations. Due to the random shifting inherent in the restoration scheme, the self-similar structure of the hierarchical cascade models is lost in the first place. This effect is best seen in the multiplier distributions for the textbook cascade model, i.e., the p model: after translational invariance in the correlation functions is restored, the multiplier distributions become scale-dependent and differ substantially from the original one. Strikingly, this is not the case once the empirically deduced β function of Ref. [11] is taken as the splitting function for the cascade model; the ''experimental'' multiplier distributions obtained after the restoration of translational invariance then stay more or less scale-invariant and equal to the original one. Moreover, the deviations from scale invariance at the very rough and the very fine scales are qualitatively the same as seen in experiment. This demonstrates that in connection with discrete multiplicative cascade models our simple scheme for the restoration of translational invariance in the spatial correlation functions seems to be consistent with experimental data for the energy dissipation field in fully developed turbulence.

Some further questions in connection with our scheme to restore translational invariance can be posed: are there other splitting functions that are more or less left invariant under this scheme, or is the experimentally deduced splitting func-

tion a kind of attractor for various different input splitting functions? What about various conditioned multiplier distributions? Work in this direction is currently in progress.

Note that the wavelet transform leads to a quasidiagonalization of the spatial second-order correlation function for the multiplicative cascade models made translational invariant. Thus wavelets approximately represent the true normal coordinates for these processes. It would be interesting to see if this finding also holds once experimental data are directly processed or other phenomenological models are investigated.

ACKNOWLEDGMENTS

M.G. and J.G. gratefully acknowledge support from DFG, GSI, and BMBF. P.L. is indebted to the Österreichische Akademie der Wissenschaften for its financial support. We thank P. Carruthers, J. Peinke, W. Scheid, and G. Soff for many fruitful discussions. We are indebted to K.R. Sreenivasan for communicating the results of his work with G. Stolovitzky prior to publication; their results inspired us to undertake the investigations presented here.

[1] V. L'vov and I. Procaccia, Phys. Rev. E **52**, 3840 (1995); **52**, 3858 (1995); **53**, 3468 (1996).
[2] B. Mandelbrot, J. Fluid Mech. **62**, 719 (1974).
[3] U. Frisch, P. L. Sulem, and M. Nelkin, J. Fluid Mech. **87**, 719 (1978).
[4] D. Schertzer and S. Lovejoy, in *Turbulent Shear Flows 4, University of Karlsruhe (1983)*, edited by L. J. S. Bradbury *et al.* (Springer, Berlin, 1984).
[5] C. Meneveau and K. R. Sreenivasan, Phys. Rev. Lett. **59**, 1424 (1987).
[6] A. Erzan, S. Grossmann, and A. Hernandez-Machado, J. Phys. A **20**, 3913 (1987).
[7] R. Lima and R. Vilela Mendes, Phys. Rev. E **53**, 3536 (1996).
[8] Z.-S. She and E. Leveque, Phys. Rev. Lett. **72**, 336 (1994).
[9] R. Friedrich and J. Peinke, Phys. Rev. Lett. **78**, 863 (1997).
[10] C. Meneveau and K. R. Sreenivasan, J. Fluid Mech. **224**, 429 (1991).
[11] K. R. Sreenivasan and G. Stolovitzky, J. Stat. Phys. **78**, 311 (1995).
[12] M. Greiner, P. Lipa, and P. Carruthers, Phys. Rev. E **51**, 1948 (1995).
[13] M. Greiner, J. Giesemann, P. Lipa, and P. Carruthers, Z. Phys. C **69**, 305 (1996).
[14] J. Giesemann, M. Greiner, and P. Lipa, Physica A (to be published).
[15] J. Pando, P. Lipa, M. Greiner, and L. Z. Fang (unpublished).